ELSEVIER

Ceramics International 29 (2003) 801–806

CERAMICS INTERNATIONAL

www.elsevier.com/locate/ceramint

A view of whitewares mechanical strength and microstructure

S.R. Bragança*, C.P. Bergmann[1]

Federal University of Rio Grande do Sul, Av. Osvaldo Aranha, 99/705, 90040-010 Porto Alegre, Brazil

Received 12 June 2002; received in revised form 9 August 2002; accepted 15 October 2002

Abstract

A traditional porcelain composed of kaolin, quartz and feldspar was formed by pressing and was sintered at temperature between 1200 °C and 1420 °C. The samples were characterized before and after sintering. A K_{IC} of 1.6 MPa $m^{1/2}$ was found for a sample fired at 1340 °C. X-ray diffraction showed the presence of mullite, quartz and glassy phase. The microstructures of samples sintered at different temperatures were analyzed by Scanning Electron Microscopy (SEM). The SEM analysis revealed that the ideal firing temperature was a consequence of glassy phase characteristics and that the maximum MOR was limited by a flaw made by quartz stress releasing. SEM images of this flaw, pore and flaw linking are showed.

Keywords: B. Microstructure-final; C. Strength; D. Porcelain

1. Introduction

The firing of porcelain promotes physico-chemical reactions responsible for the final properties of the ceramic products. In this process, it must be considered the kinetic limitations, the development of the phases, and the complexities of the microstructure. Generally, all the steps, since raw material preparation, drying conditions and firing cycle are going to have a strong influence in the product qualities. The firing cycle influence is related to the kind of furnace, firing atmosphere, maximum temperature and soaking time. All these parameters are related to quality and cost of the products.

In this work the processing parameters and the mechanical strength of porcelain were related to firing temperature with reference to the glassy phase. It was determined the fracture strength of the samples of the highest Modulus of rupture (MOR). Scanning Electron Microscopy (SEM) was used to investigate the microstructure of the samples, to explain the properties and to show which factors are limiting the specimens strength. X-ray diffraction was used to analyze the phases formed before and after firing.

A batch composition containing quartz, feldspar and kaolin was chosen. These raw materials are used in the ceramic industry. The properties and mechanical strength were studied from an industrial point of view although a scientific approach was adopted.

2. Literature survey

The work of Mattyasovszky-Zsonay [1] is very conclusive with respect to porcelain mechanical strength. Mattyasovszky-Zsonay has recommended a particle diameter of quartz of 10–30 μm and shown the influence of quartz. He disregarded the effect of mullite and explained the prestress theory.

Schüller [2] has made an analogy between quartz content and particle size explaining mechanical strength as a consequence of radial and tangential stress. Schüller found that a variation in strength occurred with a variation in quartz content. He also highlighted that the best diameter of quartz is between 15 and 30 μm.

Carty and Senapati [3] examined three hypothesis: (1) mullite, (2) matrix reinforcement and (3) dispersion-strengthening mechanism. They concluded that these three factors have an influence but the principle factor depends on the microstructure. The intrinsic flaw can be

* Corresponding author. Tel.: +55-51-33-163637; fax: +55-51-3316-3405.

E-mail addresses: saulorb@ufrgs.br (S.R. Bragança), bergmann@ufrgs.br (C.P. Bergmann).

[1] Tel.: +55-51-33-163405.

0272-8842/03/$30.00
doi:10.1016/S0272-8842(02)00234-1

either a simple pore in a sample containing a glassy phase, or a pre existing crack in a sample that does not contain a glassy phase. This is due to the presence of quartz and cristobalite.

Kobayashi et al. [4] found a high bending strength body containing a large amount of porosity. This body presented small pores distributed uniformly within the microstructure. The apparent porosity was zero although a high relative density was not obtained. Bradt (in [4]) based his explanation of the effect of quartz on the strength on Linear Fracture Mechanics. He found a K_{IC} value of 1.3 MPa $m^{1/2}$ for a body containing 10–30 μm quartz particle size.

The influence of the flux used in the fast firing of porcelain was investigated by Mörtel and Pham-Gia [5]. The author compared the properties obtained in porcelains composed of K-feldspar or Na-feldspar and concluded that they are strong influenced by the viscosity of the glass phase during firing. The glass phase depends on the kind of the flux used in the batch.

Ece and Nakagawa [6] have shown that a maximum bending strength for a 10–30 μm quartz grain size occurs after firing at 1300–1350 °C. They explained that fractures initiating from flaws were micro-cracks around quartz grains acting as links between closed pores.

Transmission Electron Microscope (TEM) and acoustic emission were used by Ohya and Takahashi [7] in order to analyze the microstructure of a porcelain body. They presented TEM micrographs showing peripheral cracks around quartz. They pointed out that these cracks are a consequence of quartz and matrix expansion mismatch during cooling from temperatures below 1000 °C.

3. Experimental procedure

The batch formulation consisted of 50% of kaolin, 25% of quartz and 25% of feldspar. Commercial quartz, kaolin and feldspar are used in the local ceramic industry. The particle sizes used were the same as is used in industry. Table 1 gives the chemical compositions of the raw material.

Table 1
Chemical composition of raw material

	Kaolin	Feldspar	Quartz
SiO_2 (%)	46.96	67.02	99.81
Al_2O_3 (%)	38.05	19.22	0.12
Fe_2O_3 (%)	0.46	0.19	0.08
MnO (%)	0.008	0.007	0.002
MgO (%)	0	0	−0.01
CaO (%)	0.02	0.06	−0.01
Na_2O (%)	0.03	3.75	0.03
K_2O (%)	1.14	9.42	0.06
TiO_2 (%)	0.03	0	0.073
P_2O_5 (%)	0.108	0.035	0.02
LOI (%)	13.2	0.3	0.1
Total (%)	*99.99*	*100*	*99.9*

The crystalline phases were determined by X-ray diffraction. The kaolin presented kaolinite [$Al_2Si_2O_5(OH)_4$] as the main phase and muscovite [$(KAl_2(AlSi_3O_{10})(OH)_2$] and illite [$KAl_3Si_3O_{10}(OH)_2$] are secondary phases. It was screened to pass 325 mesh. The feldspar contains mainly microcline ($KAlSi_3O_8$) and albite ($NaAlSi_3O_8$). It was sieved to pass 270 mesh. One hundred percent of the quartz passed through 325 mesh. This particle size is used in the majority of Brazilian industries. As a consequence, this particle size was chosen as opposed to that recommended in literature for strength maximization.

The raw materials selected were dry milled in a ball mill for 30 min to homogenize the mixture. The milling time to improve the sample properties was previously determined. Forming water was then added. The mix was granulated and pressed to sample dimensions of 8×20×60 mm.

The samples were dried for 48 h in air and then at 110 °C for 24 h in an electric furnace. After this period, the weight did not change. Then the dried pieces were weighted and measured to obtain weight loss and drying density.

The samples were fired in an electric furnace at a heating rate of 150 °C/h until they reached a temperature of between 1200 °C and 1420 °C. A soaking time of 30 min was used.

4. Results and discussion

4.1. Characterization of dried pieces

By changing the quantity of forming water added to the batch and the forming pressure it was possible to achieve the desired density of the samples (Table 2). It is very important that all the samples are about the same density so as to make a standard comparison of processing properties. The low plasticity of the batch was responsible for contraction during drying (a small

Table 2
Characterization of dried pieces

Samples for the firing temperature (°C)	Drying density (g/cm³)	Drying shrinkage (%)	Weight loss (%)
1200	1.77	−0.15	4.39
1240	1.78	−0.22	5.35
1280	1.78	−0.18	5.33
1320	1.78	−0.06	6.18
1340	1.83	−0.20	5.32
1380	1.80	−0.22	4.18
1420	1.83	−0.16	4.56

Table 3
Technical specification related to firing temperature[a]

Firing temperature (°C)	Weight loss (%)	Linear shrinkage (%)	Water absorption (%)	Apparent porosity (%)	Bulk density (g/cm^3)	Load (N)	MOR (MPa)
1200	7.4	8.2	5.50 (0.96)	12.20	2.22 (0.03)	1340	24 (2.6)
1240	7.3	10.2	2.60 (0.30)	6.00	2.35 (0.01)	1170	28 (1.5)
1280	7.4	11.5	1.50 (0.20)	3.70	2.41 (0.02)	1680	36 (3.5)
1320	7.4	12.2	0.46 (0.08)	1.10	2.47 (0.01)	1780	38 (3.5)
1340	7.3	12.2	0.34 (0.17)	0.84	2.48 (0.01)	1919	46 (2.5)
1380	7.4	11.7	0.22 (0.09)	0.54	2.42 (0.01)	1736	41 (4.7)
1420	7.6	7.25	0.59 (0.09)	1.28	2.16 (0.02)	1586	25 (3.1)

Numbers in parentheses are the standard deviations. MOR: modulus of rupture (flexural tension).
[a] Average of 10 samples taken for each temperature.

expansion occurred after pieces came out of the pressing machine).

4.2. Characterization of fired pieces

Table 3 shows the technical specification of fired pieces.

Table 3 shows a low level of water absorption, e.g. 0.46%, 0.34% and 0.22%, at 1320 °C, 1340 °C and 1380 °C respectively. Higher temperatures led to an increase in water absorption. This increase can be explained by the decomposition of oxides allowing the release of free oxygen [4,8]. Bloating also occurred at higher temperatures and led to an elevation of the apparent porosity and a decrease in the MOR as a consequence of an increased pore size.

Linear contraction, MOR and bulk density were maximized at 1340 °C. This temperature was considered to be ideal to fire this porcelain. Open porosity was found at temperatures below 1340 °C giving a poor porcelain quality. The occurrence of bloating at higher temperatures also has a deleterious effect on quality.

Fig. 1 shows that MOR increases until 1340 °C with sintering temperature. A strong glass was formed in the structure and crystalline particles were united and porosity reduced.

Porosity decreases mechanical strength by effectively reducing the materials cross sectional area. Pores can concentrate stress and reduce the flexural stress necessary to cause rupture [9]. The best criterion to indicate the reduction of porosity is bulk density. The maximum bulk density was found to occur at same temperature at which the highest MOR occurred. This confirmed the relation between MOR and density.

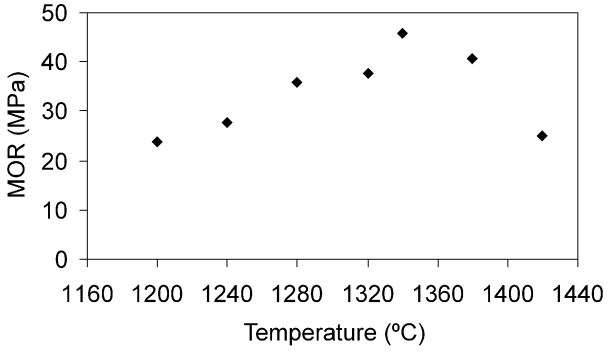

Fig. 1. Effect of firing temperature on modulus of rupture (MOR).

4.3. Fracture toughness

The values of fracture toughness (K_{IC}), fracture energy (γ) and crack length (c') are showed in Table 4. For the calculation of γ a Young modulus of 78 GPa was used [1].

The notched and unnotched samples were fired at the same time. The data from MOR measuring (Table 3) could not be used because these samples had different sizes and consequently a different area exposed to the furnace heat. Generally a larger area leads to an increase in MOR value. This explains the different values of MOR shown in Tables 3 and 4. The fired outer case has a strong influence in the mechanical strength, according to Kobayashi [4].

The mean value of K_{IC} was found to be 1.6 MPa m$^{1/2}$ (Table 4) which is a good value for porcelain. This kind of material has K_{IC} range of between 1 and 2.5 MPa m$^{1/2}$, however higher values are normally specified for electric porcelain. For example this value is higher than concrete which has a K_{IC} between 0.2 and 1.4 MPa m$^{1/2}$ [9].

4.4. Microstructure

The microstructure of the porcelain fired at 1200 °C is showed in Fig. 2 and shows an uneven texture. Even though a vitreous phase is present it is not enough to cover all the surface of the sample. A large amount of open porosity exists within the structure and explains the properties of the sample at this particular firing temperature.

The glassy phase covers the entire surface in the 1340 °C (Fig. 3). This microstructure is similar to the samples fired in the range of 1280 °C to 1380 °C. The reaction of glassy phase with the crystalline phase and

Table 4
Fracture toughness (K_{IC}), fracture energy (γ) and crack length (c')[a]

Notched samples						Non-notched samples			
Sample no.	MOR (MPa)	Load (kgf)	c (mm)	K_{IC} (MPa m $^{1/2}$)	γ (J/m^2)	Sample no.	MOR′ (MPa)	Load′ (kgf)	c' (mm)
1	15.4	7.0	1.87	1.51	14.5	11	52.4	25.5	0.257
2	19.6	9.8	1.58	1.57	15.7	12	55.7	28.0	0.224
3	28.1	13.0	1.03	1.71	18.6	13	61.8	28.0	0.180
4	19.9	9.2	1.56	1.62	16.8	14	54.3	24.8	0.238
5	19.7	9.0	1.45	1.51	14.6	15	62.3	28.9	0.177
6	30.6	14.7	0.55	1.33	11.3	16	63.2	31.1	0.172
7	22.4	10.2	1.19	1.49	14.2	17	66.1	30.1	0.156
8	27.7	13.7	1.45	2.09	27.9	18	54.6	27.2	0.234
9	18.9	9.1	1.54	1.50	14.4	19	61.4	32.1	0.182
10	24.0	12.1	1.17	1.56	15.5				
Mean	22.6	10.8	–	1.59	16.4	Mean	59.1	28.4	0.202

MOR = modulus of rupture (flexural strength).
[a] Firing temperature 1340 °C.

the entrapment of gases forming bubbles explain the small differences in the properties of the material within this temperature range.

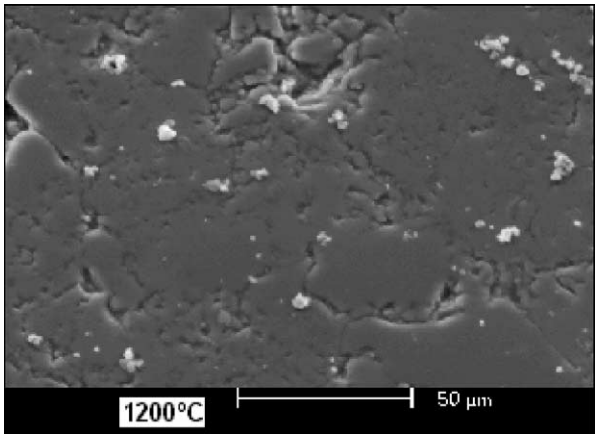

Fig. 2. SEM photomicrograph. Firing: heating rate 150 °C/h and 30 min at 1200 °C.

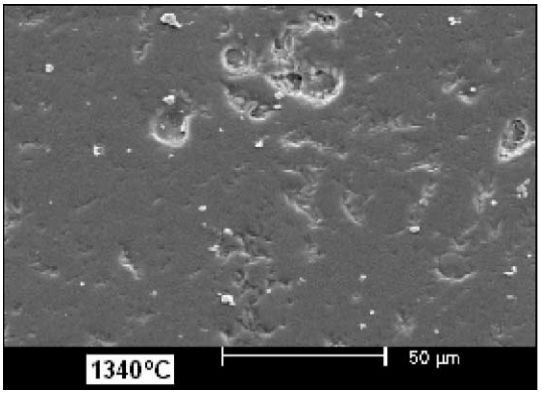

Fig. 3. SEM photomicrograph. Firing: heating rate 150 °C/h and 30 min at 1340 °C.

At 1420 °C, the size of bubbles increased as a consequence of bloating (Fig. 4). The pores showed in Fig. 4 (1420 °C) are significantly larger than the ones in Fig. 3 (1340 °C) consequently, porcelain quality was much worse. Therefore the firing above 1340 °C is unjustified according to the technical data and microstructure obtained. The opened pore in Fig. 4 is due to the pull-out of a grain during sample preparation.

In Fig. 5, it can be observed a crack in the glassy phase around a quartz grain. The quartz grain size is approximately 45 µm. This size of grain reduces the reaction of glassy phase and quartz, and only a small part of the grain could be dissolved. The quartz is responsible for initiating a flaw, which could limit the porcelain flexural strength.

Although Fig. 5 provides good information about a flaw, which might be controlling samples strength, the size showed is smaller than the theoretical size calculated previously. Fig. 6 shows the result of the microstructural analysis revealing a defect of length of 200 µm.

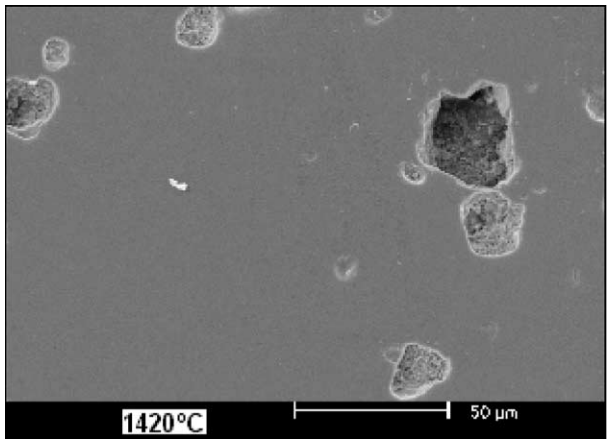

Fig. 4. SEM photomicrograph. Firing: heating rate 150 °C and 30 min at 1420 °C.

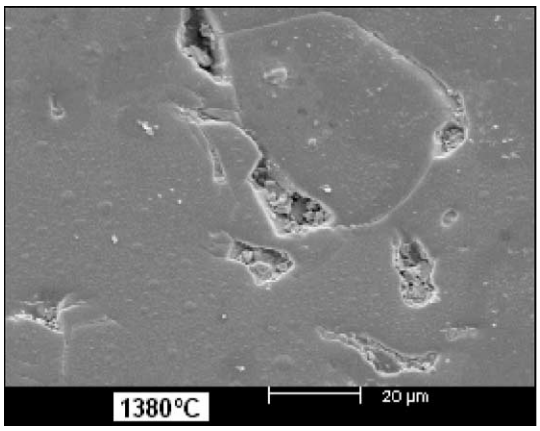

Fig. 5. SEM photomicrograph. Quartz grain is separated from glassy phase.

Fig. 6 shows a flaw of 200 µm that is made up of cracks around quartz grains. These cracks were formed as a result of quartz and matrix expansion mismatch, as postulated by Ohya and Takahashi [7]. This flaw determines the maximum possible strength of the porcelain.

An increase of porosity occurred above 1340 °C and the resistance to the propagation of the referred flaw diminished. This could explain the decrease of strength at temperatures greater than 1340 °C as bulk density and MOR are related.

4.5. Phase analysis

The analysis of the phases by X-ray diffraction showed the presence of quartz and mullite at all the firing temperatures investigated. By increasing temperature the quartz level is reduced and mullite level remains almost unchanged according to Kobayashi et al. [4], however this depends on quartz particle size [10].

Fig. 5 shows that at 1380 °C quartz particles of 45 µm can be found. This means that for commercial porcelain made up of 45 µm quartz particles, the contribution of the phases are limited as compared to particle size.

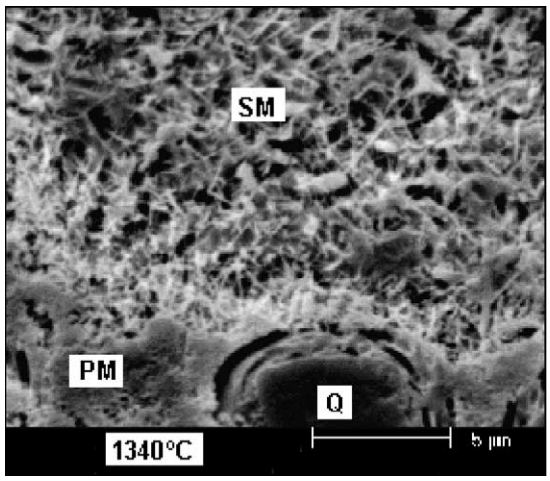

Fig. 7. SEM photomicrograph. Secondary mullite (SM), primary mullite (PM) and quartz (Q). Etched with HF 20% for 10 s.

The viscosity of the glass phase permitted the crystallization of the secondary mullite in the melt, as can be seen in Fig. 7. This phase has a strong influence in the porcelain properties, including porcelain strength [3,5].

5. Summary and conclusions

The optimum sintering temperature for the porcelain studied was 1340 °C using a heating rate of 150 °C/h and a 30 min soaking time. At this temperature the modulus of rupture and bulk density were at a maximum. The technical parameters are summarized below:

- water absorption: 0.34%
- apparent porosity: 0.84%
- bulk density: 2.48 g/cm^3

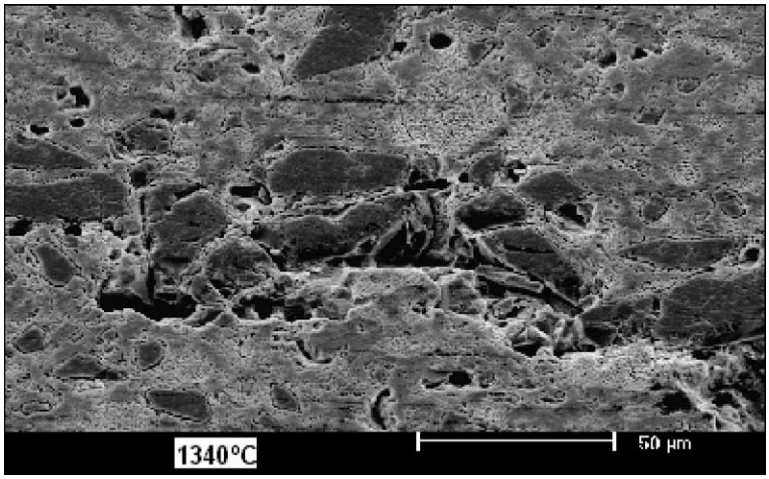

Fig. 6. SEM photomicrograph. Quartz grain forming a flaw. Etched with HF 20% for 10 s.

- linear shrinkage: 12.2%
- modulus of rupture: 46 MPa.

The analysis of the technical data showed that the modulus of rupture and the bulk density were related. The maximum strength is a result of porosity and internal flaws. Samples fired at temperatures below the ideal (1340 °C) showed open porosity. Above this temperature an increasing in closed porosity occurred due to oxygen releasing and bloating. The two types of porosity caused a decrease in sample strength.

For the ideal firing temperature (1340 °C) it was found that the fracture toughness is $K_{IC} = 1.6$ MPa $m^{1/2}$, the fracture energy $\gamma = 16.4$ J/m^2 and crack length $c = 200$ μm. These parameters are good values for a fine ceramic.

The microstructural analysis revealed that the ideal firing temperature occurs when the glassy phase covers the entire sample surface with sufficient time to react with crystalline phases. Higher temperatures were limited by the porosity increase. This porosity is a result of oxygen released from Fe_2O_3 decomposition and gas expansion in the pores.

A SEM photomicrograph image showed that a flaw size of 200 μm can be generated by the interconnection of cracks around quartz particles. This flaw is believed to be the factor that limited the porcelain strength. The difference in thermal expansion between quartz and matrix was responsible for the creation of this flaw.

The SEM microstructural analysis showed that a quartz particle of 45 μm is found at 1380 °C. Quartz grain of this dimension did not dissolve significantly and remain controlling the strength. Furthermore at this temperature, the increasing in pore size weakens the sample.

Analysis showed that the influence of the phases on mechanical strength is limited with regard firing temperature. They did not change significantly, although the quartz content was reduced with increasing temperature. However, only quartz particles of small size were dissolved and their influence is minor on mechanical strength.

References

[1] L. Mattyasovszky-Zsolnay, J. Mater. Sci. 40 (9) (1957) 299–306.
[2] K.H. Schüller, Ceramics Monographs—A Handbook of Ceramics, Verlag Schmidt GmbH, Freiburg i. Brg, 1979.
[3] M.W. Carty, U. Senapati, J. Am. Ceram. Soc. 81 (1) (1998) 3–20.
[4] Y. Kobayashi, et al., J. Am. Ceram. Soc. 75 (7) (1992) 1801–1806.
[5] H. Mörtel, K. Pham-Gia, cfi/Ber DKG 77 (5) (2000) 26–31.
[6] O.I. Ece, Z. Nakagawa, Ceram. Int. 28 (2002) 131–140.
[7] Y. Ohya, Y. Takahashi, J. Am. Ceram. Soc. 82 (2) (1999) 445–448.
[8] H.O. Gardeik, R. Scholz, Ceramics Monographs—A Handbook of Ceramics, Verlag Schmidt GmbH, Freiburg i. Brg, 1981.
[9] W.D. Callister, Materials Science and Engineering, John Wiley & Sons, New York, 2000.
[10] K.H. Schüller, Trans. Br. Ceram. Soc. 63 (2) (1967) 103–116.